Lab on a Chip

Miniaturisation for chemistry, physics, biology, materials science and bioengineering

www.rsc.org/loc

Volume 12 | Number 9 | 7 May 2012 | Pages 1563–1724

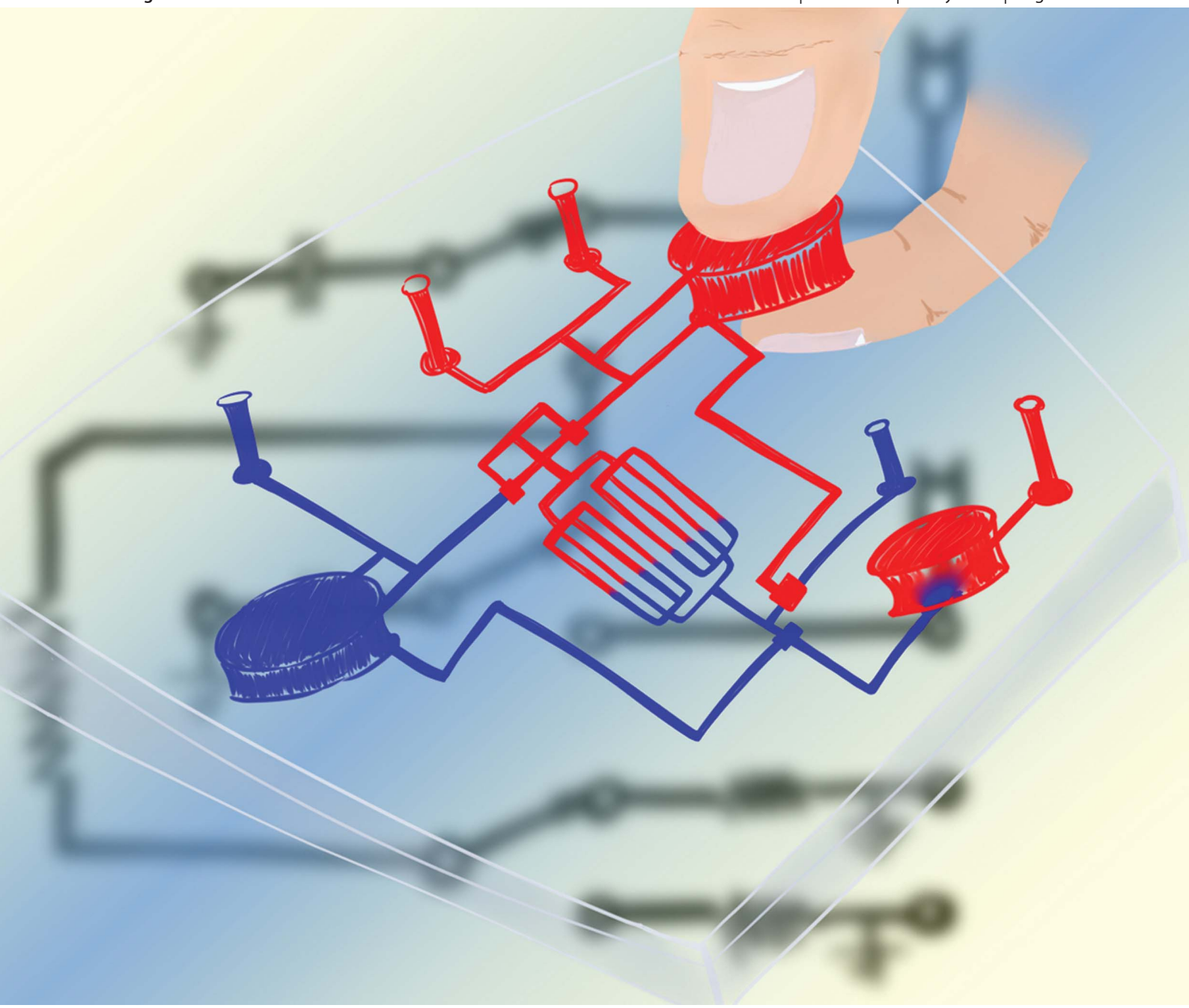

ISSN 1473-0197

RSC Publishing

COMMUNICATION

Huang *et al.*

Squeeze-chip: a finger-controlled microfluidic flow network device and its application to biochemical assays

Lab on a Chip

Dynamic Article Links

Cite this: *Lab Chip*, 2012, **12**, 1587

www.rsc.org/loc

COMMUNICATION

Squeeze-chip: a finger-controlled microfluidic flow network device and its application to biochemical assays†

Wentao Li,[a] Tao Chen,[a] Zitian Chen,[ab] Peng Fei,[a] Zhilong Yu,[a] Yuhong Pang[a] and Yanyi Huang*[ab]

Received 4th February 2012, Accepted 23rd February 2012
DOI: 10.1039/c2lc40125h

We designed and fabricated a novel microfluidic device that can be operated through simple finger squeezing. On-chip microfluidic flow control is enabled through an optimized network of check-valves and squeeze-pumps. The sophisticated flow system can be easily constructed by combining a few key elements. We implemented this device to perform quantitative biochemical assays with no requirement for precision instruments.

Microfluidic chips provide a unique approach to integrating multiple conventional laboratory works into a single device.[1,2] Recently, microfluidic technology has become a powerful tool for investigating various chemistry and biochemistry problems that are usually difficult, if at all possible, to be studied using conventional methods.[3–6] These devices are also highly valuable for medical diagnostics.[7,8] Polydimethylsiloxane (PDMS), an elastic polymer, greatly facilitates the development of microfluidics through soft lithography.[9–11] The chips are usually compact, aiming to acquire accurate results for analyzing minute amounts of samples and reducing reagent use. Precise fluid manipulation is one of the most important functions of microfluidic systems to achieve accurate results.[4,12] However, microfluidic devices have long suffered from the complex off-chip apparatus, which is usually bulky, expensive, and energy consuming. Commonly, although a microfluidic chip looks tiny and simple by itself, the whole system still requires well-trained personnel to operate, making it inconvenient to implement in remote areas, less-industrialized countries, or emergency situations.[7,13–15]

In microfluidic devices, micro-valves and pumps are critical components for the control of fluidic transportation, especially for multi-step chemical reactions or quantitative analysis. The methods of making valves and pumps have greatly facilitated the development of microfluidic technologies.[16–23] Check-valves, which not only prevent back-flow of the liquid but also provide possibilities to build the logic network of fluid, are able to simplify the whole system with fewer components needed on- and off-chip.[16,19–22,24] These check-valves, especially those using PDMS as the material for the deformable membranes, can be embedded into the device as a monolithic component, and can be linked together to perform complex logic operations.

Here, we present a finger-controlled microfluidic logic network, based on cascading embedded check-valves. We built a general-purpose colorimetric mixing chip for quantitative chemical analysis. We used this microfluidic device to demonstrate two quantitative biochemical assays for glucose and uric acid measurement. The whole experiment is conducted through finger squeezing without the need for other equipment or extra power supplies, making it a good candidate for point-of-care applications.[12]

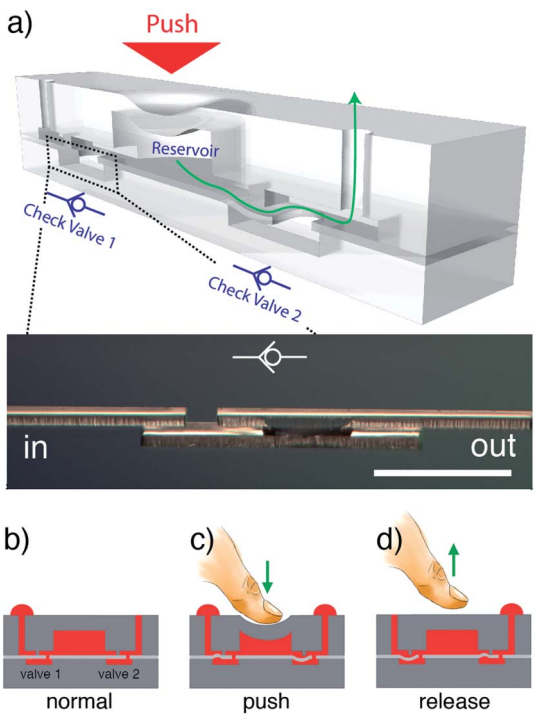

Fig. 1 The structure of a squeeze-pump. (a) The structure of a squeeze-pump that was constructed with two check-valves and a reservoir in between. The detailed structure of a single check-valve is shown in the microphotograph. Scale bar is 1 mm. (b–d) show the operation cycle of a squeeze-pump. When the reservoir is pushed, liquid will be squeezed out of the right port through valve 2. During pressure release, the reservoir is refilled through valve 1.

[a]*College of Engineering, and Biodynamic Optical Imaging Center (BIOPIC), Peking University, Beijing 100871, China. E-mail: yanyi@pku.edu.cn*
[b]*College of Chemistry and Molecular Engineering, Peking University, Beijing 100871, China*
† Electronic supplementary information (ESI) available: Figures and results. See DOI: 10.1039/c2lc40125h

Fig. 1 shows the structure of a squeeze-pump, the key component of the squeeze chips. The pump consists of two check-valves in series, and a fluid reservoir between them. Check-valves, acting as the flow diodes, only allow unidirectional liquid flow.[16,20,21,25,26] We developed a patterned surface deactivation method to help construct the check-valves in multilayer PDMS microfluidic structures (Fig. S1, ESI†). The PDMS surface became non-reactive after long-term air–plasma treatment[27–29] (Fig. S3†). Patterning is done with shadow masks made of PDMS slabs. A check-valve, similar to the design reported previous by Mosadegh *et al.*,[20] has three parts: a thin PDMS membrane layer with a hole, a top layer that contains a discontinuous channel, and a bottom layer that contains a short segment of a channel. The device was formed by bonding these three layers together but the defection membrane in the valve, whose top layer had been treated with air–plasma, could not bond to the layer above. The picture of a single check-valve is presented in Fig. 1b.

Two check-valves in each squeeze-pump ensure that the liquid can only enter the reservoir through one valve, and leave the reservoir through the other (Fig. S2†). Due to the elasticity of PDMS, when we squeeze the chip the top layer of the reservoir will deform and push the liquid out through check-valve 2 (Fig. 1a, c). When pressure is released, the liquid will be sucked in through check-valve 1 (Fig. 1a,d) to refill the reservoir. This embedded pump structure, similar to previous reported devices that transfer liquid *via* squeezes,[30–33] enables liquid sample delivery ranging from nanoliters to microliters.

We tested the correlation between the performance of a check-valve and the dimension of the valve components: the length of the gap (L), and the width (W) of the channels (Fig. S4a†). We found that the threshold to initiate the forward flow through the valve was usually lower than 1 psi for all designs. The flow resistance of the valve is relatively small, thus the flow rate heavily depends on the driving pressure. We then tested the performance of the squeeze-pumps through repetitive pushing on the reservoir using a post with controllable displacement (Fig. S5†). The flow rate is clearly related to the frequency and displacement of squeezing actions. Larger squeezing depth results in larger pumping capacity. The pump shows obvious hysteresis due to the flux limit of the valves. A proper dwell time between the adjacent squeezes greatly facilitates the pump efficiency (Fig. S4b†). The pump could deliver liquid from one nanoliter to several microliters at a time, with a CV of precision of less than 6% at 1 μL per stroke actuation. The pump is robust; it was repetitively actuated over 10^4 times without degradation of performance, and the devices were still fully functional after storage in a normal laboratory environment for 3 months.

Our check-valve-based pumping scheme allows the pressure balance tunnel to be placed remotely from the valve location. As shown in Fig. 2a, design 1 is the common structure of a check-valve that allows liquid flow from left to right. We can move the balance tunnel away from the valve area by extending the channel at the lower layer, shown as design 2. The flow direction is from left to right since the balance tunnel is connected with right part of the broken channel. Furthermore, the balance tunnel does not need to be placed on the main channel but on any branch that connects to the main channel, as shown in design 3.

We are able to create complex flow networks by rearranging the placement of valves and balance tunnels. Fig. 2b depicts an example of a pump design in which the reservoir is not between the two check-valves. The reservoir also acts as a balance tunnel, connecting the two layers of channels for the valve on the left side. When the reservoir is

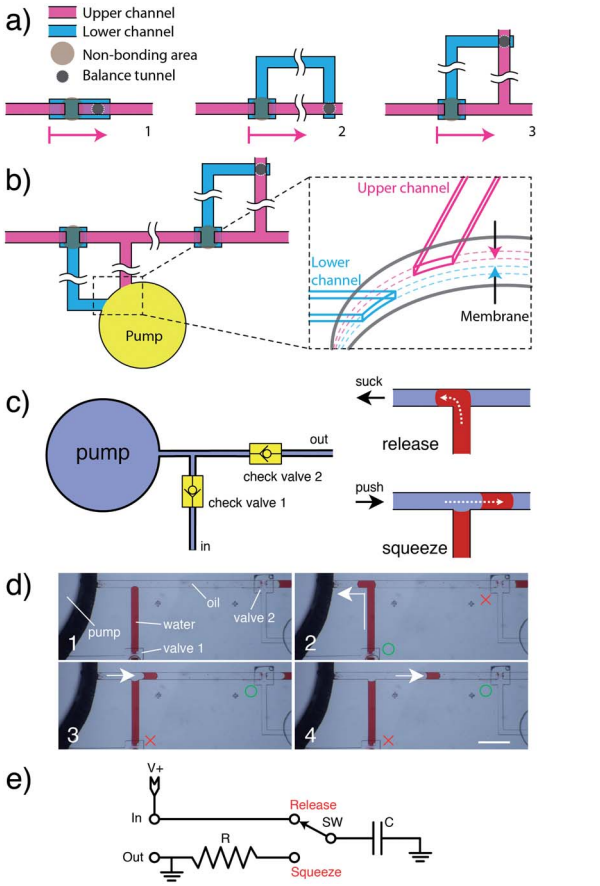

Fig. 2 The design of the squeeze-pump. (a) Various design of the check-valves. (b) A squeeze-pump that has two check-valves with remotely placed balance tunnel. (c) The design layout of a two-phase squeeze-pump for transferring small liquid plugs. (d) Microphotographs of transferring a 10 nL aqueous plug with oil as carrier. Scale bar is 1 mm. e) The electric circuit analogy of a squeeze-pump.

squeezed the liquid will be pumped out through the valve in the right side, and when it is released, it refills from the left valve. This design has the same function as the original design (Fig. 1a), but with more flexibility to arrange the channels, valves, and reservoirs.

This design also allows for applications using two immiscible liquids, as shown in Fig. 2c. The two check-valves are brought closer when the reservoir is placed on the side with a T-junction. The reservoir has been pre-filled with oil and the aqueous phase was connected to the inlet. This aqueous solution can be transferred from inlet to outlet without passing through the reservoir. The phase separation also helps to transfer small plugs with nanoliter volume. Fig. 2d shows the transfer of a 10 nL plug of dye solution by releasing (panel 2) and pushing (panel 3, 4) the squeeze-pump.

All of the above configurations of the squeeze-pump can be summarized by an electric circuit analogy, shown in Fig. 2e. In this analogy, the reservoir is a capacitor that will be charged upon releasing until full, and then discharged by squeezing. We use a simple change-over switch (single-pole double-throw) to simulate the squeeze–release actions. Flow channels, with specific flow resistance, can also be simulated as resistors in the circuit. The check-valve itself doesn't appear as an independent element in the circuit with our analogy. It has to be noticed that although this electric circuit analogy

is useful to illustrate the function of the squeeze-pump, there are a few fundamental differences between the fluidic and electric circuits. First, the polarity in the electric circuit doesn't apply to the fluidic network. Second, the ground connections are not necessary in a fluidic network. Third, the liquids can be different in the fluidic channels while the electrons are the same in electronics.

Our check-valve design, which places the balance tunnel in the downstream network of the valve, also provides great flexibility to control the fluidic routes. Downstream branches can respond selectively to the upstream pressures. The valves connected to the squeeze-pump will be closed upon the squeeze action, and hence allows the liquid to flow through certain pre-designed routes. This function produces more logical control approaches for microfluidic flow, and simplifies the design for microfluidic networks. In addition, when the valves are rationally connected to perform a specific experiment, many pressure balance tunnels can be combined together, which also reduces the complexity of chip fabrication.

Based on this concept we have fabricated a chip with 6 valves and only 3 balance tunnels for quantitative biochemical analysis (Fig. 3). In this device, valves 1 and 5 share a common tunnel, as do valves 2 and 3, and 4 and 6. This chip demonstrates the application of squeeze-pumps for liquid delivery, and control of fluid flow in and out of the device through specific routes from multiple inlets and outlets. These check-valves also serve as the route selecting elements, as explained using electric circuit analogy in Fig. 3c. The three pairs of valves, with the two reservoirs and one balance tunnel, can be simplified as a triple-pole double-throw switch in the circuit. As expected, although functions of the chip are well explained using this circuit, the circuit analogy cannot identify the difference between the liquid that is introduced from different inlets. When pump A (SW1 in the circuit) is squeezed, we drive the liquid from inlet 1 to outlet 1 through R3, a commonly connected route. Squeezing pump B (SW2 in the circuit) will drive liquid from inlet 2 to outlet 2 through R3. SW3, the analogue of the combination of valves 2, 3 and the balance tunnel between them, is one of the poles in the switch and it is passively co-operated with SW1 and SW2.

Operation of the squeeze chip for quantitative mixing of two liquids is shown in Fig. 3d. All the valves are closed in the beginning (panel 1). We can actuate (squeeze and release) pump A to fill the specific channels with one solution (red, in panel 2), and pump B with the other solution (blue, in panel 3). Both valves 1 and 5 are blocked by squeezing pump A so the red solution will flow through the metering channels and the readout chamber, to outlet 1. After the readout chamber is filled with red solution, we squeeze the pump B, which forces both valves 4 and 6 to close, to replace the solution inside the metering channels with blue solution, and the extra fluid will drip out of outlet 2. The switch between these different routes of liquid flow does not require extra control of the device. We then activate pump A to carry the blue solution in the metering channels into the readout chamber (panel 4). Although the displaced volume of each squeeze is not necessarily equal, the volume of the metering channels precisely predetermines the amount of blue solution in the readout chamber. The ratio of reactants is hence quantitatively determined by the metering channels, while the total reaction volume is set by the readout chamber. The air bubble was not a problem during the experiment since after a few firm squeezes any pre-existing bubbles were pushed out of the metering channels.

The ability of the squeeze-chips to perform quantitative reactions without using precision instruments makes this method highly suitable for point-of-care diagnostics, which usually require a simple way to handle the device. To demonstrate this ability, we carried out two colorimetric analyses on the squeeze chips to measure the concentration of glucose[34] and uric acid[35] in solutions. We set the concentration range of both analytes in clinically relevant ranges, 0–10 mM for glucose and 0–1.5 mM for uric acid. The reactions required two freshly mixed reagents (Fig. 3a, Input 1a and 1b) to react with

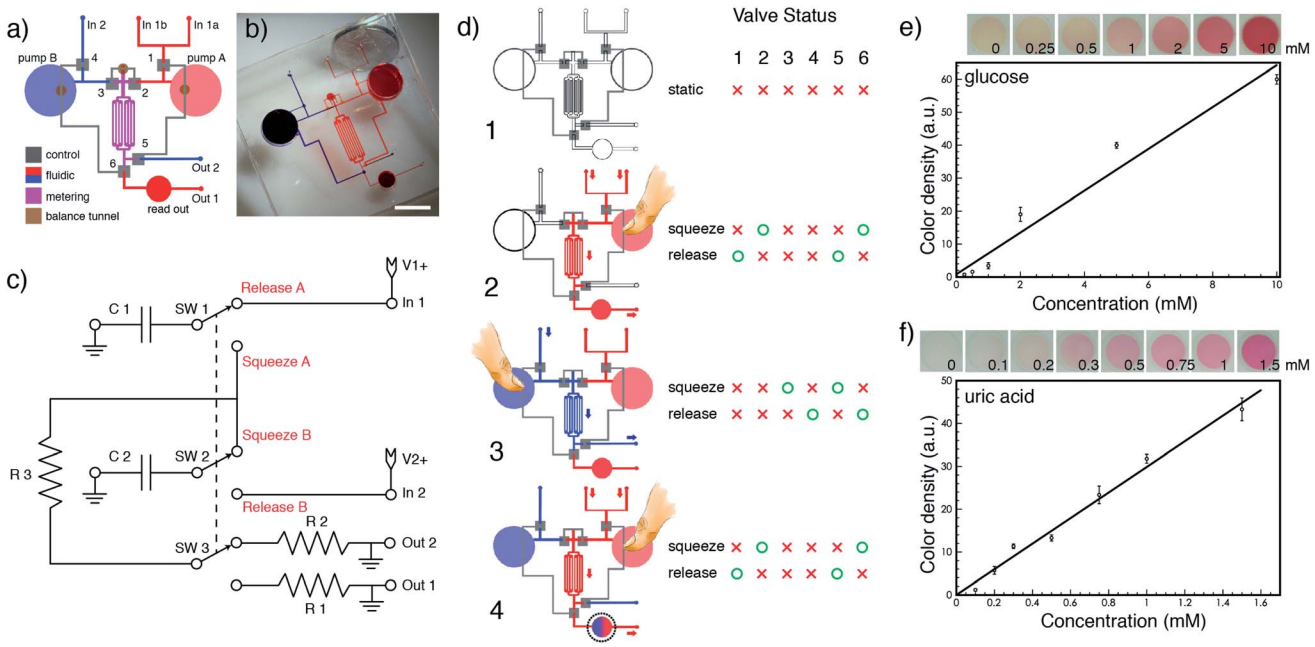

Fig. 3 The squeeze-chip for quantitative bioanalysis. (a) The design layout of the squeeze-chip with six check-valves and three balance tunnels. b) A real squeeze chip made of PDMS. Scale bar is 1 cm. (c) The electric circuit analogy of the squeeze chip. (d) The operation of squeeze-chip. the status of each valve during each squeeze-release cycle is also listed. (e) and (f) are solution-based colorimetric tests for glucose and uric acid using squeeze-chips.

samples (Fig. 3a, Input 2). The 4 mm thick readout chamber could hold liquid up to 50 μL, making it appropriate to observe the color change from the reactions by the naked eye. In our experiments we were able to detect glucose as low as 1 mM and uric acid as low as 100 μM with sample consumption less than 5 μL per test (Fig. 3e, 3f), which met the need of practical use for medical screening and quantitative diagnosis. The chips showed great tolerance for finger operation without any requirements of precision instruments. The typical operation CV is about 10∼20% in the middle of the test dynamic range for both reactions. Moreover, the colorimetric observation could be further improved by increasing the height of the readout chamber to extend the light path for absorption. This method can be applied to many other liquid phase reactions with the readout suitable for the naked eye, such as the changes in color, opacity, luminescence, and the formation of precipitation or gas bubbles. The liquid transfer mechanism can also be employed for many applications with biological samples including complex human body fluids such as whole blood.

In conclusion, we developed a technique to construct microfluidic devices with pre-determined re-configurable fluid flow networks by cascading check-valves and balance tunnels between two layers of micro-channels. These devices can be driven by simple finger-squeeze-based actuation and they perform quantitative biochemical analyses with a wide volume range from a few nanoliters to several microliters. Squeeze-chips offer a new approach to performing well-controlled micro-scale chemical and biochemical reactions, especially for point-of-care applications.

Acknowledgements

The authors thank Dr Aaron Streets, Yiran Shen, Yongfan Men, Yusi Fu, and Liang Zhao for their help and discussion. This work is supported by the National Natural Science Foundation of China (Grant No. 20890020, 90913011, and 20905004), the Ministry of Science and Technology of China (Grant No. 2011CB809106), and the Fok Ying Tung Educational Foundation.

Notes and references

1 D. C. Duffy, J. C. McDonald, O. J. A. Schueller and G. M. Whitesides, *Anal. Chem.*, 1998, **70**, 4974–4984.
2 T. Thorsen, S. J. Maerkl and S. R. Quake, *Science*, 2002, **298**, 580–584.
3 H. C. Fan, J. B. Wang, A. Potanina and S. R. Quake, *Nat. Biotechnol.*, 2011, **29**, 51–57.
4 G. M. Whitesides, *Nature*, 2006, **442**, 368–373.
5 Y. Taniguchi, P. J. Choi, G. W. Li, H. Y. Chen, M. Babu, J. Hearn, A. Emili and X. S. Xie, *Science*, 2010, **329**, 533–538.
6 P. Domachuk, K. Tsioris, F. G. Omenetto and D. L. Kaplan, *Adv. Mater.*, 2010, **22**, 249–260.
7 P. Yager, T. Edwards, E. Fu, K. Helton, K. Nelson, M. R. Tam and B. H. Weigl, *Nature*, 2006, **442**, 412–418.
8 L. Gervais, N. de Rooij and E. Delamarche, *Adv. Mater.*, 2011, **23**, H151–H176.
9 Y. N. Xia and G. M. Whitesides, *Angew. Chem., Int. Ed.*, 1998, **37**, 551–575.
10 Y. N. Xia and G. M. Whitesides, *Annu. Rev. Mater. Sci.*, 1998, **28**, 153–184.
11 Y. N. Xia, E. Kim, X. M. Zhao, J. A. Rogers, M. Prentiss and G. M. Whitesides, *Science*, 1996, **273**, 347–349.
12 A. W. Martinez, S. T. Phillips, M. J. Butte and G. M. Whitesides, *Angew. Chem., Int. Ed.*, 2007, **46**, 1318–1320.
13 N. L. Jeon, D. T. Chiu, C. J. Wargo, H. K. Wu, I. S. Choi, J. R. Anderson and G. M. Whitesides, *Biomed. Microdevices*, 2002, **4**, 117–121.
14 J. Do, S. Lee, J. Han, J. Kai, C. C. Hong, C. Gao, J. H. Nevin, G. Beaucage and C. H. Ahn, *Lab Chip*, 2008, **8**, 2113–2120.
15 M. Focke, D. Kosse, C. Muller, H. Reinecke, R. Zengerle and F. von Stetten, *Lab Chip*, 2010, **10**, 1365–1386.
16 M. A. Unger, H. P. Chou, T. Thorsen, A. Scherer and S. R. Quake, *Science*, 2000, **288**, 113–116.
17 K. W. Oh and C. H. Ahn, *J. Micromech. Microeng.*, 2006, **16**, R13–R39.
18 N. Idota, A. Kikuchi, J. Kobayashi, K. Sakai and T. Okano, *Adv. Mater.*, 2005, **17**, 2723–2727.
19 N. Futai, W. Gu and S. Takayama, *Adv. Mater.*, 2004, **16**, 1320–1323.
20 B. Mosadegh, C. H. Kuo, Y. C. Tung, Y. S. Torisawa, T. Bersano-Begey, H. Tavana and S. Takayama, *Nat. Phys.*, 2010, **6**, 433–437.
21 B. Mosadegh, H. Tavana, S. C. Lesher-Perez and S. Takayama, *Lab Chip*, 2011, **11**, 738–742.
22 X.-Q. Wang and Y.-C. Tai, 13th IEEE Int. Conf. MEMS, 2000, pp. 68–73.
23 M. L. Adams, M. L. Johnston, A. Scherer and S. R. Quake, *J. Micromech. Microeng.*, 2005, **15**, 1517–1521.
24 J. Y. Kim, J. Y. Baek, K. H. Lee, Y. D. Park, K. Sun, T. S. Lee and S. H. Lee, *Lab Chip*, 2006, **6**, 1091–1094.
25 D. C. Leslie, C. J. Easley, E. Seker, J. M. Karlinsey, M. Utz, M. R. Begley and J. P. Landers, *Nat. Phys.*, 2009, **5**, 231–235.
26 E. Seker, D. C. Leslie, H. Haj-Hariri, J. P. Landers, M. Utz and M. R. Begley, *Lab Chip*, 2009, **9**, 2691–2697.
27 D. Bodas and C. Khan-Malek, *Sens. Actuators, B*, 2007, **123**, 368–373.
28 M. A. Eddings, M. A. Johnson and B. K. Gale, *J. Micromech. Microeng.*, 2008, **18**, 067001.
29 A. Y. N. Hui, G. Wang, B. C. Lin and W. T. Chan, *Lab Chip*, 2005, **5**, 1173–1177.
30 D. Chen, M. Mauk, X. Qiu, C. Liu, J. Kim, S. Ramprasad, S. Ongagna, W. R. Abrams, D. Malamud, P. L. A. M. Corstjens and H. H. Bau, *Biomed. Microdevices*, 2010, **12**, 705–719.
31 M. Rhee and M. A. Burns, *Lab Chip*, 2009, **9**, 3131–3143.
32 J. B. Findlay, *et al.*, *Clin Chem*, 1993, **39**, 1927–1933.
33 C. Liu, X. Qiu, S. Ongagna, D. Chen, Z. Chen, W. R. Abrams, D. Malamud, P. L. A. M. Corstjens and H. H. Bau, *Lab Chip*, 2009, **9**, 768–776.
34 P. Kabasakalian, S. Kalliney and A. Westcott, *Clin. Chem.*, 1974, **20**, 606–607.
35 P. Fossati, L. Prencipe and G. Berti, *Clin. Chem.*, 1980, **26**, 227–231.

Supporting Information

Squeeze-chip: A finger controlled microfluidic flow network device and its application to biochemical assays

Wentao Li,[a] Tao Chen,[a] Zitian Chen,[a,b] Peng Fei,[a] Zhilong Yu,[a] Yuhong Pang,[a] and Yanyi Huang*[a,b]

[a] *College of Engineering, and Biodynamic Optical Imaging Center (BIOPIC), Peking University, Beijing 100871, China.*
[b] *College of Chemistry and Molecular Engineering, Peking University, Beijing 100871, China*

* Corresponding author. E-mail: *yanyi@pku.edu.cn*

1. Supporting Experimental Section

Chip fabrication. High-resolution transparency masks (Feiling Feida, Beijing, China) for each layer were printed according to the layout design. The patterns were transferred to a silicon wafers with SU-8 2050 photoresist (MicroChem, USA) by photolithography. The photoresist was spin-coated on the wafers at 3000 rpm for 1 min, resulting a ~ 50 mm thick film. PDMS (RTV 615, GE Advanced materials, CT, USA. A:B=5:1, 4mm) was casted onto the photoresist mold followed by curing in an oven at 80 ^{o}C for 15 min. PDMS slabs were peeled off to get the top layer and the bottom layer. The thin PDMS membrane was made by spin-coating a procured PDMS mixture (RTV 615, A:B=20:1, 1000 rpm for 1min) on a plastic transparency sheet, and curing in at 80 ^{o}C for 15 min. The pressure-balance holes in the membrane were punched using a biopsy puncher (2 mm in diameter). Punching was guided through the patterns on the plastic transparency sheet. To make sure holes in the membrane layer were far from main channels to prevent leaking, we designed branched channels and punched on the branched channel, as in Fig. 3a. When hole punching is finished, the bottom layer and the membrane were bonded by curing at 80 ^{o}C for 20min. We then peeled off this bonded monolithic piece from the plastic sheet (Fig. S1a, step 1a), and punched holes in the top layer (Fig. S1a, step 1b). These two pieces of PDMS slabs were covered with physical masks made from two other PDMS slabs with holes for exposing the gap positions of the valves (Fig. S1a, steps 2a and 2b). We treated the PDMS slabs with masks in air plasma (power ~ 4W, Model PR-4, Chuangweina, Beijing, China) for 20 min and then removed the PDMS masks (Fig. S1a, step 3). Finally, the three layers were aligned (Fig. S1a, steps 4a and 4b) to form the whole device completely by curing at 80 ^{o}C for 2 h (Fig. S1a, step 5). For the squeeze chips,

bigger holes (5~10 mm in diameter) were punched in the top layer to form the reservoirs.

Plasma treatment of PDMS surface. The structure of a check valve was presented in Fig. S1b. the interface between the top layer and the thin membrane had been processed so that the two could not be bonded at that part. The whole device is a monolithic piece after bonding, as shown in Fig. S2, except the pre-treated part that was not bonded. This unbonded part of the membrane, well attached to the break point of the upper channels when no forward pressure is applied, is the most critical part of the check valve. Through a small hole in this membrane, the upper channel and the lower channel are connected. This tunnel balances the pressures between the outlet port and the lower channel. When the liquid is driven forward (Fig. S2a,b) the membrane will deflect downward to open the valve, while driven backward (Fig. S2c,d) the membrane will deflect upward and block the liquid flow. The surface modification has been realized by a longtime air-plasma treatment using masks (made by PDMS) to protect the untreated region. Extremely overdosed oxygen plasma treatment would destroy PDMS surface's flatness, generate cracks, and make the material crispy and fragile (Fig. S3). To bond two PDMS blocks, we usually treat two PDMS surface with 4W air plasma for 30 sec. When the treatment lasts more than 2 min, the bonding strength will dropped quickly. When the treatment lasts more than 10 min, nanometer-size cracks start forming on the surface, making it not bond to each other.

Performance test of check valves. We designed check valves with different gap length and channel width. The valves were linked to compressed air with Tygon tubing. The pressure of compressed air was controlled with a needle-valve. We applied pressure from 1 to 10 psi to the inlet of each passive valve, and collect the DI water passed valves within 1 min. All the tubes were in the same height level to make sure no extra pressure difference between inlet and outlet. Each data in Fig S4a is the mean from three different devices with identical values of L and M.

Performance test of the squeeze-pumps. The performance of the pump was tested with a homemade apparatus shown in Fig. S5. A stepped motor was used to drive a post to push/squeeze the pump. The diameter of the reservoir is 10 mm and the height is 3 mm. The inlet and outlet of a pump were connected to water containers with Tygon tubing. The liquid levels in both containers were kept the same. We use a computer to control the squeezing displacement, frequency, and dwell time of each action. We squeezed and released the pump for 100 times and collect the water passed through the pump. Each data in Fig. S4b is obtained from three independent measurements. During the measurement, we drove out all air bubbles from the channels and the reservoir to avoid the affection from different compressibility between air and water.

Glucose and uric acid detection. Glucose and uric acid were purchased from Alfa Aesar. The test kits for glucose and uric acid were purchased from Beijing shouyi clinical scientific center. The kit includes phosphate buffer, 4-amino-antipyrine, uricase, 2,4,6-tribromo-3-hydroxy acid, peroxidase, and stabilizers. The uric acid reaction was based on an uricase end-point method. This

solution-based reaction generates hydrogen peroxide that can be further converted to chromophore with the help of peroxidase. The similar principle has also been applied to the chromogenic reactions for test glucose. The hydrogen peroxide produced from glucose by glucose oxidase action will lead to chromophore formation.

2. Supporting Figures

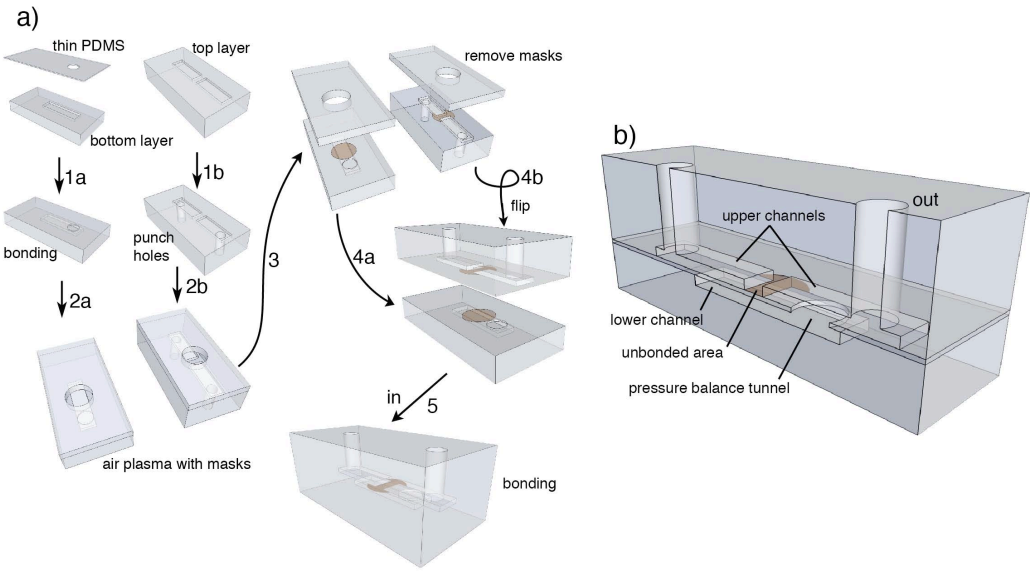

Fig. S1 The monolithic PDMS check valves. a) Fabrication of a check valve. b) Structure of a check valve. A deformable membrane section, created by oxidization of the PDMS surface through air plasma treatment, is the key component of the valve.

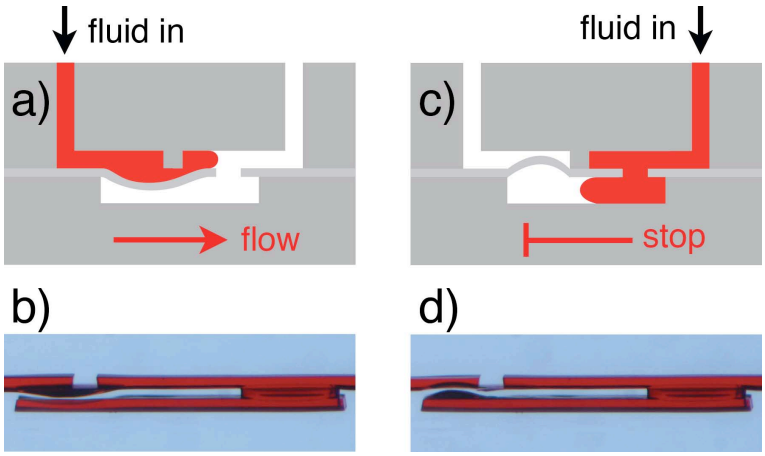

Fig. S2 The function of a monolithic PDMS check valve. a) The valve status under forward hydrodynamic pressure (side view). The valve is open for forward direction (left to right). b) The microscopic photograph of a valve under forward pressure. The channels are filled with red solution and the deformation of the thin PDMS membrane is clearly observed. c) The valve status under backward hydrodynamic pressure (side view). The valve is closed for backward direction (right to left). d) The microscopic photograph of a valve under backward pressure.

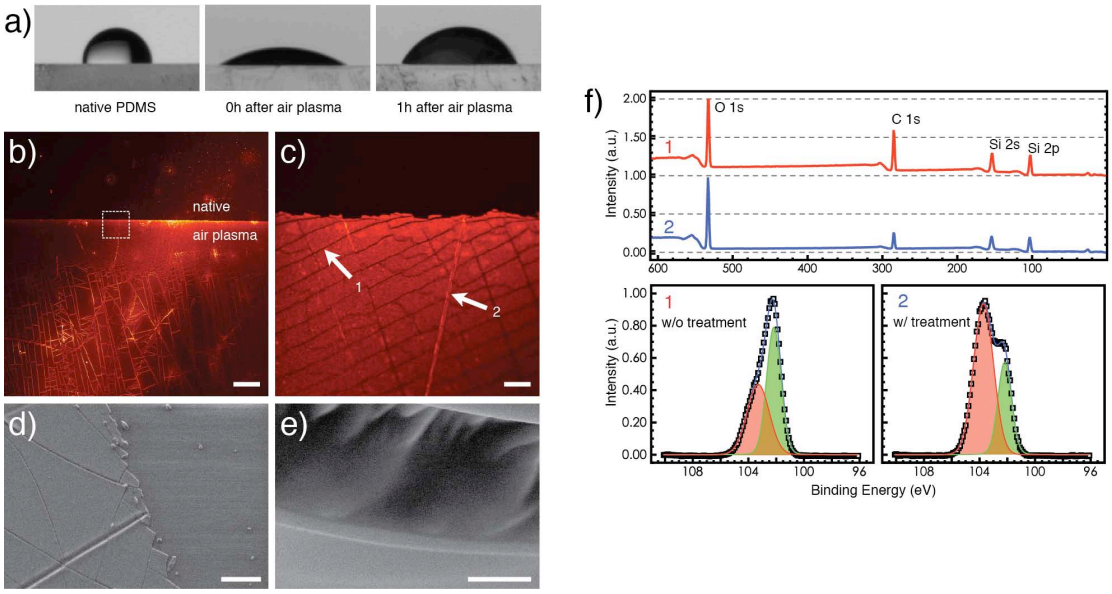

Fig. S3 Surface deactivation of PDMS. a) Contact angels of PDMS surface before and after air plasma treatment. b) Confocal image of the PDMS surface, with and without air plasma treatment. We stain the PDMS by soaking a slab in Rhodamine B solution. Scale bar is 100 μm. c) The high magnification image shows the cracks with different width (arrows). Scale bar 10 μm. d) and e) are SEM pictures of the cracks on PDMS surface. Scale bars 15 μm and 250 nm, respectively. f) XPS spectra of PDMS surfaces before (1) and after (2) the air plasma treatment. The fitted results of the Si 2p peaks show the composition of silica (red) and polymer (green) forms.

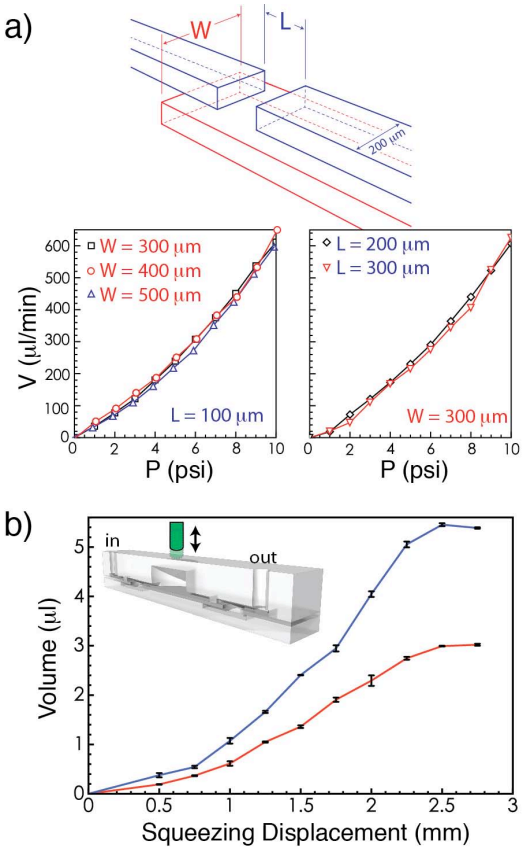

Fig. S4 a) The flow velocity of water through the valves is not sensitive to structure variation. b) Volume per squeeze measured from a chip (reservoir is 1 cm in diameter and 3 mm thick). 1s dwell time between the squeezes (blue line) offers better pump efficiency than continuous squeezes (red line).

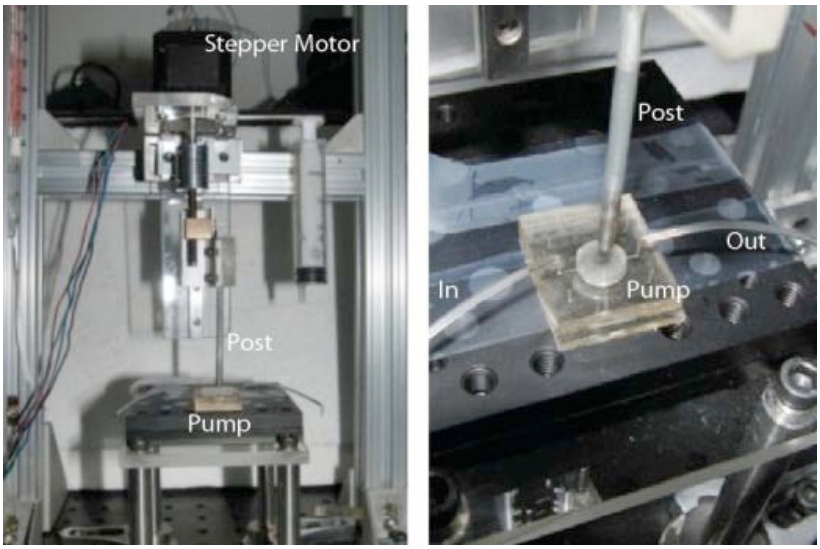

Fig. S5 The homebuilt apparatus for performance test of a pump. A computer was used to control the stepper motor, which drove the dome-headed post to push the chip. The diameter of the metallic post is 2mm, and the squeezing/releasing speed is 1.2 mm/s.

3. Supporting Movies

(1) Side view of the open and close statuses of a check valve under the forward and backward pressures, respectively.

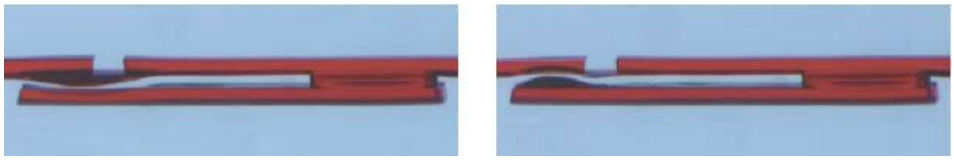

(2) Nanoliter range aqueous plugs (red) are transferred by squeezing an oil-filled reservoir (left) connected with two check valves through a T-junction (also see Fig. 4b).

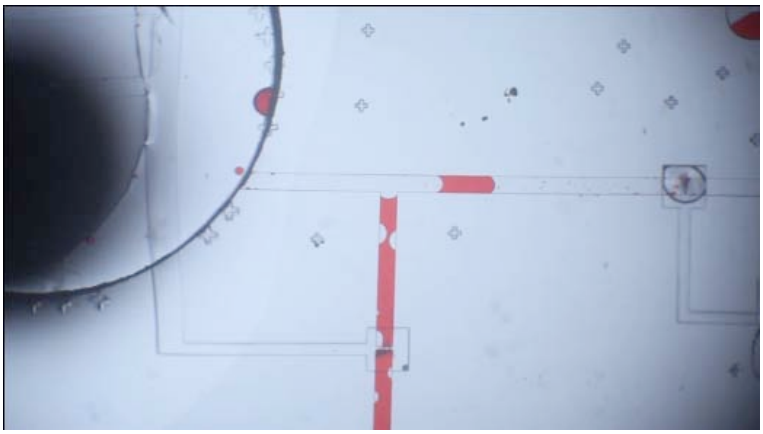

(3) Operation of a squeeze chip. Dyes are used to demonstrate the liquid flow driven by the pump actuations.